

1 INTRODUCTION

The energy demand of pump systems accounts for a major part of the primary energy demand worldwide. Studies show, e.g., that in 2015 11.3 % of the total energy demand in Germany (572 PJ) is attributable to mechanical drives in pumps, cf. [4] and [5]. To reduce this high share, it is mandatory to design and implement efficient and reliable booster stations.

In past investigations of pump systems – such as booster stations for high-rise buildings – primarily the individual components have been the subject of interest: the pumps are considered as isolated elements and their efficiency is measured, and possibly optimized, at a single operating point, the best efficiency point (BEP) [6]. A slightly broader scope is investigated when measuring a pump's *Minimum Efficiency Index* (MEI): two additional operation points at overload and at partial load, respectively, are used for assessing the pump's energy efficiency. This procedure is part of an European Standard for energy-efficiency evaluation of water pumps [7].

Both of the mentioned methods are related to the so-called *Product Approach*, since the focus lies on the product itself and it is not taken into account whether the product is used efficiently in the system. While these approaches have led to efficiency improvements, there is still a discrepancy between the real-world operating conditions and the considered test scenarios: data for booster stations in [8] show that the peak volume flow is only required in 1 % of the time. Furthermore, Jaberg estimates in [1] that – due to oversizing or varying loads – 90 % of all pumps operate at partial load and not at their BEP.

For this reason, the *Extended Product Approach* was developed within the scope of energy efficiency guidelines of the European Union [9]. In addition to product efficiency, the energy-efficient application is also taken into account. A load profile is considered, which links volume flow and pressure demands with corresponding time profiles. The energy consumption of the Extended Product (pump and electric motor) considering these load profiles yields the Energy Efficiency Index (EEI) [10].

Further development leads to the *System Approach*: not the individual components are subject of investigation, but the interaction of various components that results in the overall system [11]. In [1], this approach is motivated by considering the energy consumption: In a pumping system, only 15 % of the energy is dissipated in the pumps; the major part is dissipated in the surrounding system. In [6] it is estimated that 75 % of the energy saving potential is attributed to the system due to (i) better system control, (ii) better

system design and (iii) selection of better sized pumps, and that only 7.5 % of the saving potential can be realized by using more efficient pumps.

However, exploiting the optimization potential at system level is challenging: A huge amount of different possible components, configurations and operational parameters has to be taken into account. In real-world applications, this leads to an overwhelming number of design choices and configuration and control possibilities. Based on this insight, a method for investigating and optimizing the system as a whole was investigated in a joint project of TU Darmstadt, MLU Halle and KSB SE & Co. KGaA. By applying the methodology Technical Operations Research (TOR) to pumping systems, significant optimization potential could be identified [3].

TOR is a guideline for system optimization which considers the interaction of different system components and is thus a holistic approach in the sense of a system approach. By applying optimization algorithms from discrete mathematics, one is able to explore the multitude of all possible system configurations. With TOR, out of all options, a system configuration is found which – given the model accuracy and the considered degrees of freedom – yields the desired performance in an optimal way, i.e. with highest efficiency or lowest life cycle cost. Global optimality is guaranteed, i.e. there can be no better system [12].



Figure 1: Steps of the TOR methodology [12].

The steps of the TOR-methodology are shown in Figure 1. The first step is part of the decision phase: This phase involves clarifying of (1.) the function (*What do I need the system for?*), (2.) the objective (*Which measures or properties of the system should be optimized?*) and (3.) the degrees of freedom and constraints of the system (*What are the boundary conditions and the available components?*). In the following action phase, (4.) a mathematical mixed-integer optimization model is derived and solved using state-of-the-art solvers. The solution is then (5.) verified using simulation tools such as Modelica [13] and (6.) validated by

experimental investigations. Final step (7.) is the implementation of the real system.

Apart from the TOR methodology, mathematical optimization methods for technical systems have been used in many different applications, e.g. in process engineering [14] or for energy networks [15]. A detailed description of mathematical optimization methods applied to water distribution networks is given in [16].

In this work, we focus on the water supply for high-rise buildings using booster stations. These systems are used to provide sufficient water pressure in the upper floors and are characterized by a high portion of operation in partial load. Furthermore, the required pressure increase is dominated by the geodetic height.

The regulations for the planning and operation of booster stations are specified in DIN 1988-500 [17]. In conventional systems, parallel pumps of the same type are used. The possibility to respond to fluctuating loads is given by switching pumps on/off (cascade control) or, if frequency inverters are installed, by adjusting the rotational speed of one or multiple pumps.

Previous work has shown that the restriction of the topology to (i) parallel pumps [18] [19] and/or (ii) pumps of the same type [20] leads to unnecessary high energy and investment costs. Furthermore, recent investigations show that additional saving potentials can be exploited by decentralizing pumps, i.e. by supplying floors individually [16] [21]. In addition, the consideration of uncertainties during the planning phase, e.g. by anticipation of pump failures, is increasingly gaining interest [16] [22].

While we could experimentally validate optimization results of the TOR methodology for a smaller example, cf. [23], there is no publication in which the TOR methodology is used comprehensively for central booster systems without limiting the topology, and by including simulative verification and experimental validation.

In this paper, we present the application of all steps of the TOR-methodology for a downscaled, centralized booster station. This includes data collection for modeling, global optimization as well as validation by means of simulations and experiments.

2 TEST RIG FOR BOOSTER STATIONS

We developed a test rig, which models a booster station for high-rise buildings. All floors of the downscaled building are supplied by a central booster station in the basement, and dimensions, components and load cases were scaled as shown in Table 1. It is not possible to achieve complete similitude, but all substantial characteristics have been kept.

Table 1: Comparison of booster stations for real buildings and downscaled booster station at the test rig.

	REAL BUILDING	TEST RIG
geodetic height difference	45 m	5 m
Number of floors (sinks)	15	5
open/closed system		open system
medium		water
load cases		mainly partial load
		centrifugal pumps
type of pumps	special pumps for booster stations	heating circulation pumps
Pressure loss due to friction compared to geodetic height		$\alpha_R \approx 52 \%$
maximum volume flow	20 m ³ /h	5 m ³ /h

The test rig is 6 m high and consists of five outlets with a height difference of 1 m each (cf. Figure 2). From a tank at ambient pressure, the water is pumped to the outlets. Up to six pumps, connected in any topology (e.g. combination of parallel and serial connections), are used as a booster station. At each outlet, representing the different floors, there is a volume flow sensor, control valve and inspection glass. The water flows back into the tank due to gravity via a drainpipe at ambient pressure.

A total of 13 different heating circulation pumps (centrifugal pumps) are available. The rotational speed of each pump is controlled and the power consumption and pressure increase is measured. Different load cases can be realized by the different heights of the floors in combination with the control valves.

Similar to real systems, the booster station is mainly operated at partial load and the ratio of pressure losses due to friction and geodetic heights is approx. 52 % (cf. Chapter 3.1).

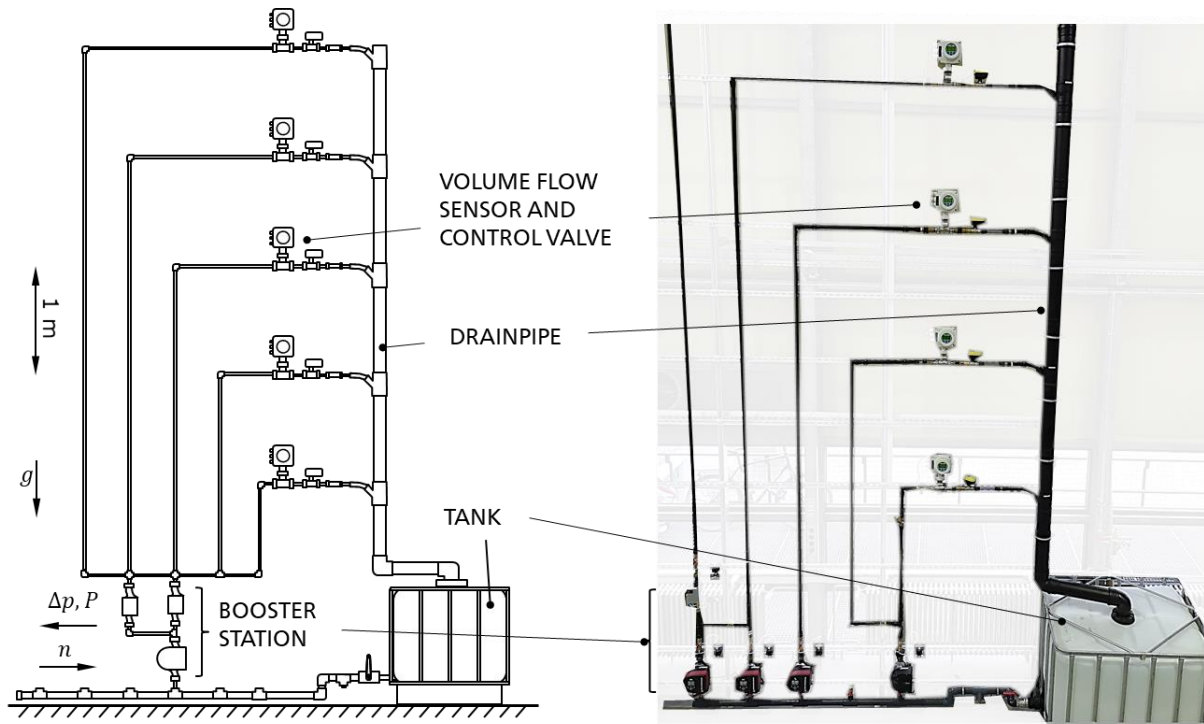


Figure 2: Test rig for flexible pumping systems. Left: Schematic illustration, right: photography

3 OPTIMIZATION MODEL

In this chapter, we derive an optimization model for the booster station in our test rig according to the TOR methodology. The importance of using optimization methods versus brute force is shown in Figure 3: at the test rig, 10^{102} decisions regarding piping and 10^5 decisions regarding both pump selection and placement have to be made. This results in a total of 10^{112} possibilities for the design of the booster station. In addition, the optimal rotational speed of the pumps has to be selected. This number of variants is no longer comprehensible with classical methods, making the use of mathematical optimization methods necessary.

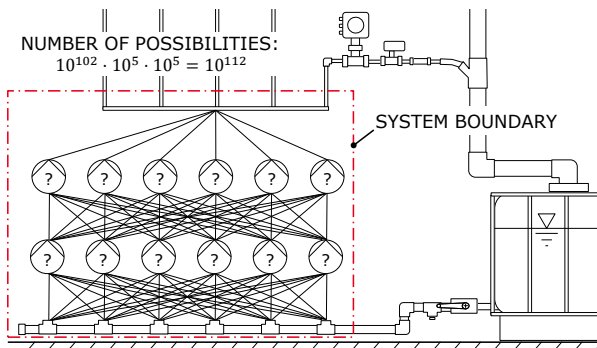


Figure 3: Possible number of different topologies for the booster station at the test rig.

3.1 Function

The function of a DEA is to satisfy the water demand on all floors. The water demand and thus the load of the DEA are represented in the form of load profiles, whereby each load case is defined by volume flow, pressure increase and time share. Hirschberg presents in [8] a load profile for booster stations derived from the time series of measured volume flows in real buildings. In order to reduce the complexity, the respective adjacent load cases are combined and thus the number of load cases are reduced by half (cf. Figure 4).

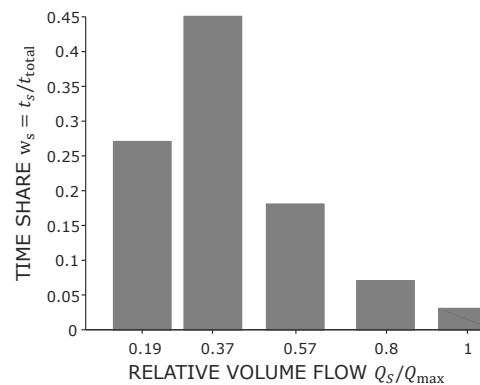


Figure 4: Time shares for different relative volume flows defining the reduced load profile for real booster stations according to [8] with the volume flow Q_s in load case s and the maximum volume flow Q_{max} .

To use this distribution for the test rig, the maximum volume flow Q_{max} has to be scaled. In order to

obtain comparability to real booster stations, Q_{\max} is selected in such a way that the influence of friction in the test rig equals that in real buildings. The share of the pipe network resistance is estimated in [8] as:

$$\alpha_R := \frac{\Delta p_{\text{friction}}}{\Delta p_{\text{geodetic}}} = \frac{f(Q_{\max})}{f(H)} \approx 52 \%. \quad (1)$$

The required pressure increase due to the geodetic height of $H = 5 \text{ m}$ is:

$$\Delta p_{\text{geodetic}} = H \rho g = 49\,050 \text{ Pa}. \quad (2)$$

To determine $\Delta p_{\text{friction}}$, a model of the test rig is necessary, describing the pressure losses as a function of the volume flow. It is assumed that the volume flow demand is the same on all floors. The pressure losses in the inlet, the rising pipes and the outlet are taken into account. The losses within the booster station are highly dependent on the interconnection of pumps and are located within the system boundaries of the optimization. For this reason, these losses cannot be simply integrated and are neglected. The calculation of pressure losses is based on Bernoulli's stationary equation

$$\Delta p_{\text{friction}} = \frac{1}{2} \rho \zeta_{\text{in}} \left(\frac{Q}{A_{\text{in}}} \right)^2 + \frac{1}{2} \rho (\zeta_{\text{rising}} + \zeta_{\text{out}}) \left(\frac{Q/5}{A_{\text{out}}} \right)^2 \quad (3)$$

with the pressure loss coefficients ζ , estimated as a function of the installed pipes and fittings according to the manufacturer's specifications or literature data. Based on Eqs. (1) to (3), the maximum volume flow is estimated to $Q_{\max} = 4.564 \text{ m}^3/\text{h}$.

The relative load profiles shown in Figure 4 are used to determine the absolute volume flow demand Q_s of the different load cases. The necessary pressure increase of each load case is calculated combining Eqs. (2) and (3) to $\Delta p_{\text{booster},s} = \Delta p_{\text{friction},s} + \Delta p_{\text{geodetic},s} = f(Q_s, H)$. The load cases are summarized in Table 2.

Table 2: Load cases of the booster station

Load case s	Time share $w_s = t_s / t_{\text{total}}$	Volume flow Q_s in m^3/h	Pressure increase $\Delta p_{\text{booster},s}$ in m
1	27 %	0.87	5.12
2	45 %	1.67	5.39
3	18 %	2.60	5.90
4	7 %	3.63	6.68
5	3 %	4.56	7.60

3.2 Objective

The objective of the optimization is a cost-optimal fulfilment of the requirements defined by the load cases. In addition to the investment costs, which are given by the purchasing costs of the pumps $c_{\text{pump},r}$, the average energy costs C_{energy} over a period of t_{total} years are taken into account. The objective function reads

$$C = t_{\text{total}} \cdot c_{\text{elect.}} \cdot \sum_{s \in S} \sum_{r \in R} w_s P_{r,s} + \sum_{r \in R} x_r c_{\text{pump},r} \quad (4)$$

with the energy price $c_{\text{elect.}}$, the time share $w_s = t_s/t_{\text{total}}$, the power consumption $P_{r,s}$ of pump r in scenario s and the purchase decision variable x_r . The latter equals 1 if pump r is purchased and 0 if not.

This is a multi-criteria optimization problem where energy and investment costs have to be balanced. Both costs are summarized in a single objective function (4), in which the time period t_{total} is a weighting factor.

3.3 Physical Modeling and Playing field

The degrees of freedom of the system configuration are described by a catalogue of optional components and constraints which model the possible interconnections between these components. The booster station is considered as a system with the boundaries shown in Figure 3.

Goal of the optimization is to determine the optimal

- purchase decision for pump models from a set of 13 pumps,
- switch-on time of pumps in each load case (maximum of six simultaneously),
- rotational speed of each pump in every load case,
- connection of the selected pumps in each load case.

In order to make these decisions optimally, their impact on function (volume flow promotion) and objective (energy and investment costs) has to be described. Therefore, physical models are necessary.

The modeling of the pump characteristics (H - Q and P - Q characteristics) is one of the most important steps to describe the system behavior. Basically,

two data sources are available: (i) measurements and (ii) manufacturer data. In this contribution, we focus on the latter one. We use the known affinity laws, cf. [24], to describe the relationship between the pressure increase and power consumption of a pump and its rotational speed and volume flow, and choose polynomials to fit the data.

constant power consumption, independent of volume flow and rotational speed, caused by electrical components like the control and transmitter unit.

In order to determine the constants, a multivariate fit is performed using the manufacturer's data. The correlation between data points according to the manufacturer and the regression is shown in *Figure 5*. Further physical models are the volume flow conservation and pressure increase within the booster station. These are described in greater detail in the next Section.

3.4 Mathematical Model

The mathematical model is an adjusted version of the ones described in [23] and [25]. It consists of an objective function (cf. Eq. (4)), several constraints and the decision variables. The constraints ensure that the physical laws mentioned in Section 3.3 are satisfied and that the solution is feasible, e.g. that the load cases are fulfilled. The optimal assignment of the variables is determined within the optimization, e.g. the optimal pump speed or purchase decision. Therefore, the system has to be described by analytical equations.

A graph $G = (V, E)$ with nodes V and edges E is used to describe the superstructure of the system, i.e. all possible topologies. It consists of one source node v_Q and one sink node v_S , as well as two nodes per possible pump. Each edge connecting two pump nodes represents a possible pump. Different connections are realized by adding further edges to the graph (in the following referred to as activation of an edge). The graph of all possible connections for three pumps is shown in *Figure 6*.

Figure 5: Data points according to manufacturer and regression according to Eqs. (5) and (6) for Grundfos Magna3 25-60. Top: H-Q characteristics ($R_{adj}^2 = 99.95\%$); bottom: P-Q characteristics ($R_{adj}^2 = 99.9\%$)

A quadratic and a cubic approach are used for the H-Q characteristic the P-Q characteristic, respectively. Using the affinity laws, this yields:

$$H(Q, n) = a_1 Q^2 + a_2 Q \tilde{n} + a_3 \tilde{n}^2 = f(Q^2, Q \tilde{n}, \tilde{n}^2) \quad (5)$$

$$P(Q, n) = b_1 Q^3 + b_2 Q^2 \tilde{n} + b_3 Q \tilde{n}^2 + b_4 \tilde{n}^3 + b_5 = f(Q^3, Q^2 \tilde{n}, Q \tilde{n}^2, \tilde{n}^3) \quad (6)$$

with the relative speed $\tilde{n} = n/n_{\max}$ and the constants a_i and b_i . The constant b_5 does not result from the hydraulic affinity laws. It describes a

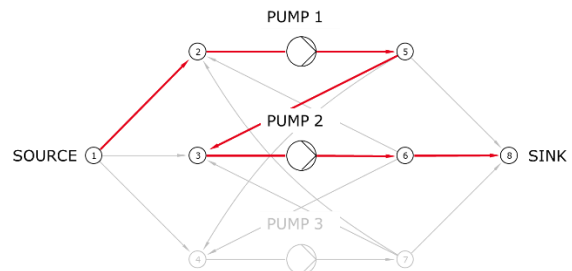


Figure 6: Graph of all possible connections in the case of three available pumps. Active edges are shown in red, resulting in a serial connection of pump 1 and 2.

The physical laws are defined using this graph. This includes the volume flow conservation in each load case s at each pump node $V_P = V \setminus \{v_Q, v_S\}$:

$$\sum_{i \in V} Q_{i,j,s} = \sum_{i \in V} Q_{j,i,s} \quad \forall j \in V_P \quad \forall s \in S. \quad (7)$$

Furthermore, a volume flow $Q_{i,j,s}$ on an edge (i, j) is only possible if this edge is active ($y_{i,j,s} = 1$):

$$Q_{i,j,s} \leq Q_{\max} \cdot y_{i,j,s} \quad \forall i, j \in E, \quad (8)$$

$$\forall s \in S,$$

$$y_{i,j,s} \in \{0,1\}.$$

The pressure difference $H_{j,s} - H_{i,s}$ between two inlet i and outlet j of an active pump (i, j) is given by the pump characteristic $H_{i,j,s} = f(\text{pump type}, \tilde{n}, Q_{i,j,s})$ according to. Eq. (5):

$$H_{j,s} - H_{i,s} \leq H_{i,j,s} + (1 - y_{i,j,s})H_{\max} \quad (9)$$

$$H_{j,s} - H_{i,s} \geq H_{i,j,s} - (1 - y_{i,j,s})H_{\max}$$

$$\forall i, j \in V_p \quad \forall s \in S$$

with the normalized rotational speed $\tilde{n} = n/n_{\max}$. The pressure losses within the booster station (e.g. due to elbows or fittings) are not considered. This would require a much more precise modeling of the interconnections – each fitting would have to be considered as an additional edge in the graph – increasing the complexity and computation time significantly.

Further constraints such as the maximum number of six pumps that can be operated at the same time, the interrelation between the purchase decision on the activity of pumps and the satisfaction of the load cases are not explained here for reasons of clarity.

4 OPTIMIZATION RESULTS

The optimization model was implemented in MATLAB, using the toolbox YALMIP [26] with the OPTI toolbox [27] serving as an interface to various solvers. For this work, the MINLP solver SCIP 5.0 [28] was used. It can solve nonlinear, non-convex problems to proven global optimality. Compared to the use of MILP solvers (as done in [18] and [25]), there is no need for a piecewise linearization of the pump characteristics.

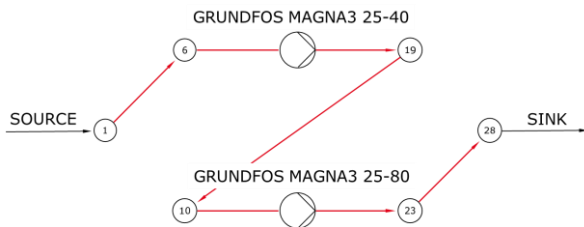


Figure 7: Optimal booster station for an operation time of 10 years and no restriction on the topology.

The optimal solution for an operation time of $t_{\text{total}} = 10$ years is shown in Figure 7. In each load case, the pumps "Grundfos Magna3 25-40" and "Grundfos Magna3 25-80" are chosen and connected in series.

To be able to compare this result with other layouts, in a next step, the topology options were fixed to parallel connections of a number of pumps of the same type – as it is state-of-the-art for booster stations. Yet, the selection of the pump type, the switch-on time of each pump, and the rotational speed were degrees of freedom and were optimized, cf. Figure 8. Due to the optimization of these three aspects, one can still expect efficiency advantages over conventional systems, even for the restricted topology options.

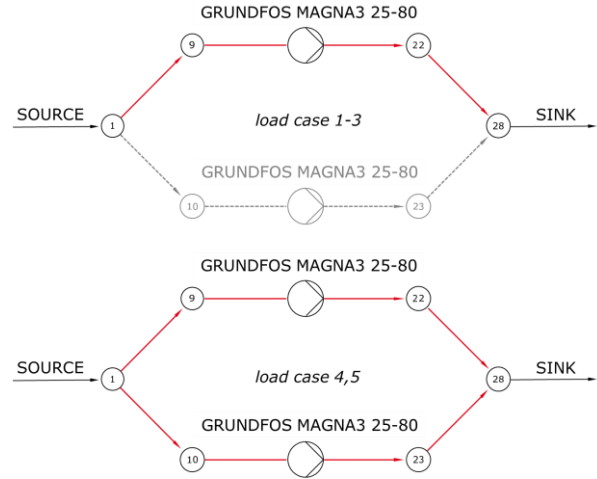


Figure 8: Optimal booster station for an operation time of 10 years and restriction to parallel pumps of the same type. In load case 1-3 (top), only one of the two pumps is running, whereas in case 4 and 5, both pumps are running (bottom).

A comparison of the solutions in Table 3 reveals that for an unrestricted topology, investment costs can be reduced by 12.3 % and energy consumption can be reduced by 6.5 %, compared to a system of parallel pumps. However, the computing time for finding optimal solutions for the optimization model without topology restrictions increases significantly.

Table 3: Comparison between the performance of the solution with and without topology restrictions.

	Unrestricted topology	Parallel pumps of same type
Total costs in €	3015.58	3403.40
Investment costs in €	2510.98	2863.52
Average power consumption in W	65.22	69.78
Computing time in s	49326	0.83

5 VALIDATION

When modeling a superstructure of various possible system variants and using mathematical optimization methods, one has to balance accuracy and required computing time to calculate the solution. Due to the inherent complexity of the underlying optimization models, it is often required

to simplify and approximate the technical and physical details. For this reason, a validation of the optimization results is mandatory. The purpose is to confirm the function (*Is the volume flow demand achieved?*), the objective (*Does the energy consumption of the system match the value predicted in the optimization?*) and the feasibility in practice. In the following, the solutions of the optimization are compared with the results of simulation models and experimental investigations and deviations are discussed. In general, the level of detail increases from optimization towards simulation and experiment. However, also complexity and effort increase.

The computed optimal system configuration is mapped to a simulation model and the test rig. This comprises the selection of the pumps, connections, switch-on times and rotational speeds for the different load cases. Since one optimal topology defined by the mathematical graph can be realized by different layouts in reality, we select the layout with the lowest possible pressure losses within the booster station (e.g. as few fittings and bends as possible).

Validation by means of simulations allows to consider more details and to investigate different solutions with little effort. Therefore, we use the modeling language Modelica [13], in which 0-dimensional models are used to simulate fluid systems, cf. Figure 9.

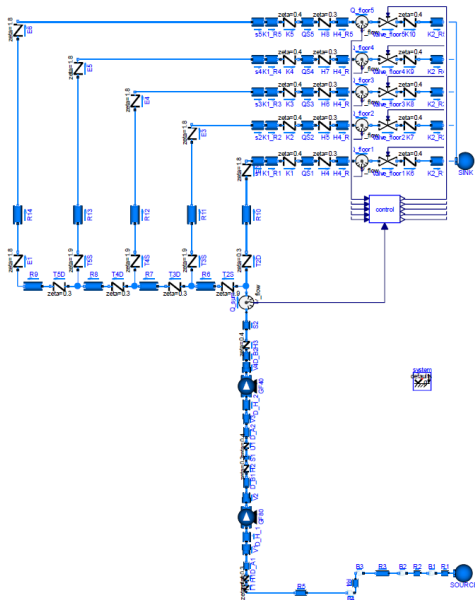


Figure 9: Modelica model of solution shown in Figure 7. The models are based on the components of the test rig.

Similarly, for an experimental validation, optimal system variants computed by the optimization model are set up on the test rig, and volume flow

and energy consumption in different load cases are measured.

In order to examine the satisfaction of the required function, i.e. the fulfillment of the volume flow demand, the volume flow in all floors, averaged with the probability w_s , is computed. The results of optimization, simulation and experiment are shown in Table 4.

Table 4: Results of optimization, simulation and experiment of solution with and without restriction to parallel pumps of the same type.

	Optimization		Simulation		Experiment	
	Unrest. Top.	Rest. Top.	Unrest. Top.	Rest. Top.	Unrest. Top.	Rest. Top.
Average volume Flow in m³/h	1.85	1.85	1.28	1.1	1.29 ± 0.04	1.43 ± 0.04
Average power consumption in W	65.22	69.78	60.59	60.93	61.7 ± 1.77	66.6 ± 1.70
Average efficiency in %	41.83	40.02	40.19	33.52	37.86	32.82
Expected total costs in €	3015.6	3403.4	3036.23	3508	3068.4	3521.5

Our validation shows, that the volume flow provided by the booster station is significantly lower than the one predicted by the optimization model, making it lower than the demand. This difference is higher in the experimental validation than in the simulation.

One reason for this are the pressure losses within the booster station that were neglected in the optimization model. The simulation allows a closer analysis: In particular, the cross-sectional change before and after an installed pump results in pressure losses, which can be confirmed experimentally. In future investigations it is possible to integrate these losses into our optimization model by taking them into account in the pumps' characteristic curves.

The differences in power consumption listed in Table 4 are not representative due to the discrepancies in the volume flow values. For this reason, the average efficiency of the system is calculated for optimization, simulation, and experiment, respectively:

$$\eta_{mean} := \sum_{s \in S} w_s \cdot \frac{\sum_{i \in V_p} P_{hydr,i,s}}{\sum_{i \in V_p} P_{elect,i,s}} \quad (10)$$

Due to the higher pressure losses compared to the ones modeled in the optimization program, the pumps will operate at higher partial load in reality. While this reduces the electrical power consumption, the overall average efficiency is lower.

The expected energy costs are calculated using the average efficiency. For the unrestricted topology, energy costs computed by experimental data are 9.5 % higher than predicted by the optimization, yielding 1.7 % higher total costs (energy + invest) for the assumed operation time. The experimental data for the topology restricted to parallel connections shows a slightly higher volume flow, which is closer to the value predicted by the optimization. However, compared to the experimental set up with unrestricted topology, the power consumption is higher, which leads to a lower average efficiency. Overall, the experimental data for the restricted topology yields a total costs that are 3.5% higher than expected according to the optimization result.

6 CONCLUSIONS

In this contribution we have presented the application of all steps of the TOR methodology for planning a central booster station with unrestricted options for interconnecting the pumps. This compromises the definition of the system function, the optimization goal, and the degrees of freedom in the system topology. Moreover, we have presented the physical modeling of the system based on a real test rig. An optimization program was developed and its solution was compared to a reference solution with a topology restricted to parallel connections, only. Both solutions were validated using (i) a Modelica simulation and (ii) a modular test rig.

The results show that the necessary approximations in the optimization models cause non-negligible discrepancies between optimization and simulation and experiment. The results of the simulation match the experimental data better than the ones of the optimization model. This can be attributed to the higher level of detail in the simulation. However, only by using the presented optimization models, an investigation of the full solution space including all system variants is feasible. The general approach to planning optimal systems should therefore be based on what the TOR method suggests: First, optimization methods should be used to search the full solution space for optimal system topologies. The underlying optimization models will inevitably be more coarse than simulation models, due to the higher amount of degrees of freedom (unknown system topology vs. known system topology). The optimal solutions found should therefore be validated by simulation and experiment.

In our investigations we noticed, that the total costs for energy and investment computed based on experimental data exceed the ones computed within the optimization model by 1.7 % and 3.5% for the unrestricted and restricted topology, respectively. Moreover, we noticed an average difference in the volume flows delivered by the pumps in reality, compared to the values predicted by the optimization model. Due to this discrepancy in performance, adjustments in operation are necessary in the real system, e.g. an increase of the pumps' rotational speed. This is a non-trivial task for complex topologies and will be investigated in future work. In addition, methods are required to consider necessary approximations and uncertainties during the planning phase.

7 ACKNOWLEDGEMENTS

The presented results were obtained within the research project "Exact Global Topology-Optimization for Pumping Systems", project No. 19725 N/1, funded by the program for promoting the Industrial Collective Research (IGF) of the German Ministry of Economic Affairs and Energy (BMWi), approved by the Arbeitsgemeinschaft industrieller Forschungsvereinigungen "Otto von Guericke" e.V. (AiF). We want to thank all the participants of the working group for the constructive and close collaboration. Moreover, we want to thank Deutsche Forschungsgemeinschaft (DFG, German Research Foundation) for partially funding this research under project number 57157498 (SFB 805).

8 REFERENCES AND BIBLIOGRAPHY

- [1] H. Jaberg, "Energieverbrauch, Energieersparnis und Energieverschwendung in Pumpen und Systemen," *chemie&more*, 02 2015.
- [2] B. Stoffel, "Assessing the Energy Efficiency of Pumps and Pump Units," Elsevier, 2015.
- [3] C. Hamkins, P. Pelz, L. Altherr, W. Zimmermann and B. Saul, "Abschlussbericht zum BMWi-geförderten Verbundprojekt "Hocheffiziente Pumpensysteme" (HEP) im Rahmen des 5. Energieforschungsprogramms der Bundesregierung, 03ET1134," KSB SE & Co KGaA , Frankenthal , 2017.
- [4] M. Blesl and A. Kessler, *Energieeffizienz in der Industrie*, Springer Vieweg, 2017.
- [5] C. Rhode, "Erstellung von Anwendungsbilanzen für die Jahre 2013 bis 2017 - Studie für die Arbeitsgemeinschaft Energiebilanzen e.V. (AGEB)," Fraunhofer-

- Institut für System-und Innovationsforschung (ISI), Karlsruhe, 2018.
- [6] B. Went, "Energy legislation and the European pump industry - The systems approach to reducing carbon emissions," *World Pumps*, pp. 52-55, 05 2008.
- [7] *EN 16480: Pumps - Minimum required efficiency of rotodynamic water pumps*, 2016.
- [8] R. Hirschberg, "Lastprofil und Regelkurve zur energetischen Bewertung von Druckerhöhungsanlagen," *HLH Lüftung/Klima,Heizung/Sanitär, Gebäudetechnik*, 2014.
- [9] N. Bidstrup, M. Teepe, G. Berge and G. Ludwig, "Extended Product Approach for Pumps," in *Europump*, 2014.
- [10] S. Lang, G. Ludwig, P. F. Pelz and B. Stoffel, "General Methodologies of Determining the Energy-Efficiency-Index of Pump Units in the Frame of the Extended Product Approach," in *8th International Conference on Energy Efficiency in Motor driven Systems*, Rio de Janeiro, Brasilien, 2013.
- [11] Europump, "European Pump Industry - Energy Commitment," Brussels, 2015.
- [12] P. F. Pelz and U. Lorenz, "Besser geht's nicht! TOR plant das energetisch optimale Fluidsystem.," *chemie & more*, 01 2014.
- [13] Modelica Association, "Modelica® - A Unified Object-Oriented Language for Systems Modeling, Version 3.4," 2017.
- [14] J. Kallrath, "Solving Planning and Design Problems in the ProcessIndustry Using Mixed Integer and Global Optimization," *Annals of Operations Research* 104.1, p. 339–373, 2005 .
- [15] J. Kallrath, P. M. Pardalos, S. Rebennack and M. Scheidt, *Optimization in the Energy Industry*, Berlin, Heidelberg: Springer, 2009.
- [16] L. Altherr, P. Leise, M. E. Pfetsch and A. Schmitt, "Resilient Layout, Design and Operation of Energy-Efficient Water Distribution Networks for High-Rise Buildings Using MINLP," *Optimization and Engineering*, 2019.
- [17] "DIN 1988-500:2011-02 - Technische Regeln für Trinkwasser-Installationen," 2011.
- [18] P. Pelz, U. Lorenz, T. Ederer, S. Lang and G. Ludwig, "Designing Pump Systems by Discrete Mathematical Topology Optimization: The Artificial Fluid Systems Designer (AFSD)," in *International Rotating Equipment Conference*, Düsseldorf, 2012.
- [19] J. Weber and U. Lorenz, "Optimizing Booster Stations," in *Proceedings of the Genetic and Evolutionary Computation Conference Companion (GECCO'17)*, New York, 2017.
- [20] P. Pöttgen and P. F. Pelz, "The best attainable EEI for Booster Stations derived by Global Optimization," in *International Rotating Equipment Conference*, Düsseldorf, 2016.
- [21] P. Leise, L. C. Altherr and P. F. Pelz, "Energy-Efficient Design of a Water Supply System for Skyscrapers by Mixed-Integer Nonlinear Programming," in *Operations Research Proceedings 2017*, Berlin, 2017.
- [22] M. Hartisch, A. Herbst, U. Lorenz and J. Weber, "Towards Resilient Process Networks - Designing Booster Stations via Quantified Programming," in *3rd International Conference on Uncertainty in Mechanical Engineering (ICUME 2018)*, Darmstadt, 2018.
- [23] L. C. Altherr, T. Ederer, U. Lorenz, P. F. Pelz and P. Pöttgen, "Experimental Validation of an Enhanced System Synthesis Approach," in *Operations Research Proceedings 2014: Selected Papers of the Annual International Conference of the German Operations Research Society (GOR)*, Aachen, 2016.
- [24] I. Karassik, J. Messina, P. Cooper and C. Heald, *Pump Handbook*, p. 2.19-2.22, New York: McGRAW-HILL, 2001.
- [25] P. Pöttgen, T. Ederer, L. C. Altherr and P. F. Pelz, "Developing a Control Strategy for Booster Stations under Uncertain Load," *Applied Mechanics and Materials* , pp. 241-246, 2015.
- [26] J. Löfberg, "YALMIP : A Toolbox for Modeling and Optimization in MATLAB," in *In Proceedings of the CACSD Conferenc*, Taipei, Taiwan, 2004.
- [27] J. Currie and D. I. Wilson, "OPTI: Lowering the Barrier Between Open Source Optimizers and the Industrial MATLAB User.," in *Foundations of Computer-Aided Process Operations*, Savannah, Georgia, USA, 2012.
- [28] A. Gleixner, L. Eifler, T. Gally, G. Gamrath, P. Gemander, R. L. Gottwald, G. Hendel, C. Hojny, T. Koch, M. Miltenberger, B. Müller, M. E. Pfetsch, C. Puchert, D. Rehfeldt, F. Schlösser, F. Serrano, Y. Shinano and J. Viernickel, "The SCIP Optimization Suite 5.0," *Optimization Online.*, 2017.